JOURNAL OF SOLID STATE CHEMISTRY 4, 345–350 (1972)

The Preparation and Properties of Single Crystals of the 1*S* and 2*S* Polymorphs of Tantalum Disulfide*

LAWRENCE E. CONROY AND KONDAYOOR RAGHAVAN PISHARODY

Department of Chemistry, University of Minnesota, Minneapolis, Minnesota 55455

Received June 25, 1971

Tantalum disulfide crystallizes in several different polymorphs, all of which consist of close-packed sulfur atom layers with the tantalum atoms occupying the interstices in alternate layers. Single crystals of two TaS_2 polytypes, one containing Ta atoms in octahedral vacancies and one in which the Ta atoms are situated in trigonal prismatic sulfur environment, have been prepared by chemical transport, and their electrical, magnetic, and optical properties have been examined. The 1*S* (octahedral) polytype is a diamagnetic semiconductor of very low resistivity, whereas the 2*S* (trigonal prismatic) form exhibits metallic properties. The metallic characteristics of 2*S*-TaS_2 are consistent with energy band models that have been applied to other layered transition metal disulfides, but the semiconducting 1*S*-TaS_2 is not adequately described by these models.

Introduction

Tantalum disulfide crystallizes in a number of polytypes (*1*) all of which are characterized by layer-type structures in which the metal atoms are situated in layers between alternate sulfur layers. Each S—M—S layer is bonded to adjacent such layers by relatively weak Van der Waal forces, so that these substances cleave readily along the layer dimensions. Hägg and Schönberg (*2*) observed four distinct phases of TaS_2 which they designated as α (a C6 type structure in the Strukturbericht classification), β (a C27 type), γ (a C19 type), and δ (a new structure type). The α form, which has the $Cd(OH)_2$ structure, can take up extra tantalum atoms in the vacant layers to form nonstoichiometric phases up to a composition of $TaS_{1.6}$. The other forms are stoichiometric. In 1962, Jellinek (*1*) showed that the four forms were stacking polytypes consisting of close-packed sulfur layers in which the tantalum atoms occupied either octahedral sites or trigonal prismatic sites. Jellinek designated as type 1*S* the form in which tantalum occupies octahedral sites in alternate layers of a *hcp* sulfur array. This form is the $Cd(OH)_2$ structure having the space group $P\bar{3}m$. In the β form, labeled type 2*S* by Jellinek, the metal atoms are situated in a trigonal prismatic environment with roughly twice the *c*-axis repeat distance found in the 1*S* type, 12.1 Å instead of 5.8 Å. Type 2*S* can be described in space group $P6_3/mmc$. A third form, not classified by Hägg and Schönberg, is labeled type 3*S* in the Jellinek classification and also contains Ta atoms in a trigonal sulfur environment. However, in this case the stacking order produces rhombohedral symmetry (space group *R3m*) and involves a three-layer repeat distance. ($c = 17.9$ Å on a hexagonal basis.) The δ form of TaS_2 is rhombohedral (space group *R3m*) with a six-layer arrangement of the S–M–S sandwich. Referred to a hexagonal cell the *c*-axis is 35.85 Å. In this phase Ta atoms occupy both octahedral and prismatic sites. Schönberg's γ form is reported by Jellinek to be a nonstoichiometric form of the 3*S* structure type.

Recently, Wilson and Yoffe (*3*) have reported the optical properties of some of these tantalum polytypes and conclude that the 1*S* phase must be nonmetallic, whereas the 2*S* type is metallic. Both of these polytypes have been reported (*4*) as superconductors below 0.7°K.

All of the previous electrical studies on the TaS_2 polytypes were carried out on polycrystalline

* Based upon a thesis presented by K. R. Pisharody to the Graduate School of the University of Minnesota in partial fulfillment of the requirements for the Ph.D. degree. This research was supported in part by the United States Army Research Office—Durham.

powders. Our research was directed toward the preparation of single crystals of the TaS_2 polytypes so that the powder data could be confirmed or corrected. By utilizing chemical transport techniques for crystal growth, it was possible to prepare and characterize large single crystals of the 1*S* and 2*S* phases. This paper reports the results of this study.

Experimental

Starting materials were tantalum metal powder, 99.9%, obtained from United Mineral and Chemical Corp., resublimed 99.99% sulfur, and reagent grade 99.9% iodine.

Polycrystalline tantalum disulfide was prepared by sealing a stoichiometric mixture of the elements in evacuated silica tubes and heating it for one week at 900°. The product was a black free-flowing powder. This material was then recrystallized by a chemical transport technique (*5*), using iodine as the transport agent. Samples of the TaS_2 powder, weighing 1–5 grams, were sealed in evacuated silica ampules along with resublimed iodine (4 mg I_2/ml ampule volume). Various sizes of ampules, ranging from 15 to 25 cm in length and 2.5 cm in diam were employed. The techniques for loading and evacuating the ampules has been previously described (*6*). The transport ampule was heated in a two-zone tube furnace that provided independent temperature control and programs for each zone. Initially both zones were heated to 1000° and held at that temperature for 12 hr. The charge zone was kept at 1000° while the growth zone was cooled to 800° at a rate of 10°/hr. This overheating of the growth zone is designed to minimize multiple nucleation of crystals. Transport was carried out over the gradient 1000–800° for one week. Under these conditions large, metallic-gray, single crystals of 2*S*-TaS_2, 1–2 cm across × 50 microns thick, were formed in the growth zone. Only the 2*S* polytype was formed under these conditions.

It was found possible to induce the growth of the 1*S* form of TaS_2 by introducing a small quantity (0.2 mg/ml) of the isomorphous tin disulfide into the transport ampule. With SnS_2 present, transport from 1000–800° yielded roughly equal quantities of yellow 1*S*-type crystals and metallic-gray 2*S*-type crystals. The two forms could easily be separated manually because of the large crystal size.

Analysis for tin contamination was carried out by polarography (*7*) and by X-ray fluorescence. No detectable quantities of tin were found in either type of crystal by these techniques.

Chemical Analysis

Quantitative analysis for tantalum and sulfur were carried out on each batch of crystals that were used in the electrical, magnetic, and optical measurements. For the tantalum determination (*8*, *9*), crystals of TaS_2 were fused with $NaHSO_3$ and the cooled cake was dissolved in a hot aqueous solution of 4% ammonium oxalate. The solution was transferred to a 100-ml volumetric flask, to which was added 10 ml of pyrogallol solution (15 g pyrogallol in 60 ml water and 5 ml of 1:1 sulfuric acid). After dilution to volume, the absorbance of this solution was read at 400 mμ on a Cary Model 14 spectrophotometer. The standard solution was prepared in an analogous way from 99.9% Ta_2O_5. Determination on known samples indicated an accuracy of ±0.5% for this method.

For sulfur analysis, a sample of TaS_2 was fused with a large excess of Na_2O_2 or with a Na_2O_2–Na_2CO_3 mixture. The cooled cake was dissolved in water, acidified with HCl, and the sulfate was precipitated with excess $BaCl_2$. Attempts to analyze sulfur by oxidation to SO_2 were unsuccessful, apparently because tantalum oxide catalyzes the conversion to SO_3. Results on known samples were about 6% low by the SO_2 method.

Results Calcd. for TaS_2: Ta 73.83, S 26.17%. Found for 1*S*-TaS_2, Ta 73.1, S 26.1%. Found for 2*S*-TaS_2: Ta 73.7, S 26.2%.

X-Ray diffraction data were obtained on powdered samples using a Debye–Scherrer camera and filtered Cu*K*α radiation. Lattice parameters were refined by a least squares program adapted to Cohen's (*10*) method.

Magnetic susceptibilities were determined by the Faraday method, using a Cahn microbalance. The single-crystal samples weighed approximately 5 mg. Both platinum metal and $Hg[Cd(SCN)_4]$ were employed as calibration standards. Temperatures were measured with a Cu–constantan thermocouple.

Electrical resistivities were measured on single crystals by the Van der Pauw (*11*) method. Because of the crystal dimensions, measurements could only be made perpendicular to the *c*-axis, parallel to the metal–sulfide layers. Electrical contacts to a crystal were made with conducting silver paint at the perimeter of the platelet. All measurements were made in He atmosphere. Reproducibility was within ±5% on metal calibration standards.

Specular reflectance spectrophotometric data were recorded in the 2000–25,000 Å region using single crystal samples. Samples were mounted on a Barnes Model 126 Micro Specular unit installed

TABLE I

CRYSTALLOGRAPHIC DATA ON TaS_2 CRYSTALS

	Color	Space group	Lattice constants: This work a (Å)	This work c (Å)	Jellinek (*1*) a (Å)	Jellinek (*1*) c (Å)
1*S*	yellow	$P\bar{3}m$	3.365 ± 0.002	5.853 ± 0.002	3.36	5.90
2*S*	metallic-gray	$P6_3/mmc$	3.316 ± 0.002	12.070 ± 0.002	3.315	12.10

in a Cary model 14 spectrophotometer. Neutral absorbers in the reference compartment were used to control the intensity balance. White, unpolarized light at normal incidence was employed. The faces of cleaved crystal were used in the unpolished state, because microscopic examination showed the natural surfaces to be more uniform than polished ones. Reflectivities were measured for crystal-air $[n_m(D) = 1.000]$ interfaces. Because of difficulties in standardizing the double-beam optics, only relative absorbances are reported.

Results and Discussion

Chemical transport provided a very satisfactory means of preparing single crystals of two of the TaS_2 polytypes. Although the 2*S* phase transported most readily, the presence of small quantities of SnS_2 catalyzed the formation of the 1*S* form to the extent that roughly equal quantities of both forms could be obtained in the presence of this reagent. In contrast with the experience of Van Maaren and Schaeffer (*12*), we obtained the 1*S* form only in the presence of the SnS_2 or by seeding the growth zone with 1*S*-TaS_2 crystals after the high temperature pretreatment of the silica ampules. The large, very thin platelets were suitable for electrical and optical measurements without further preparation other than washing with CCl_4 to remove surface iodine.

Crystallographic data are shown in Table I, along with the data of Jellinek (*1*) on these two forms. The identity of our crystals with the 1*S* and 2*S* forms identified by Jellinek are clearly indicated.

Magnetic susceptibility measurements showed the 1*S* form of TaS_2 to have an extremely small susceptibility that was beyond the sensitivity (10^{-7} emu/g) of the apparatus throughout the temperature range from 78 to 300°K. The 2*S* form was weakly paramagnetic with a mass susceptibility (uncorrected) ranging from $\chi_g = +0.2 \pm 0.1 \times 10^{-6}$ emu/g at 300°K to $\chi_g = +0.3 \pm 0.1 \times 10^{-6}$ emu/g at 78°K. No literature data are available for comparison with these values.

The electrical conductivity data are shown in Fig. 1 for the 1*S* form and in Fig. 2 for the 2*S* form. The 1*S*-TaS_2 is a semiconductor of very low resistance. A rapid increase in conductivity becomes evident above a temperature of 320°K, the slope in that region corresponding to an activation energy of approximately 0.1 eV. Below that temperature extrinsic conductivity, probably the result of excess metal atoms in the crystals, is the dominant mechanism. The proclivity for the layer disulfides to crystallize with excess metal is well documented (*3*). The 2*S* phase is metallic. The slight break in the slope of the 2*S*-TaS_2 conductivity plot near 260°K was examined thoroughly and found to be reproducible on different crystals and with temperature cycling. The resistivity of the 1*S* form was 3.7×10^{-3} ohm-cm at 295°K and 10.1×10^{-3}

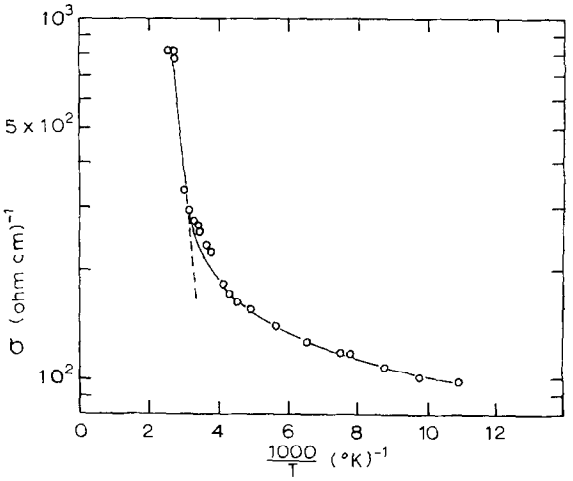

FIG. 1. Conductivity of 1*S*-TaS_2 as a function of reciprocal temperature.

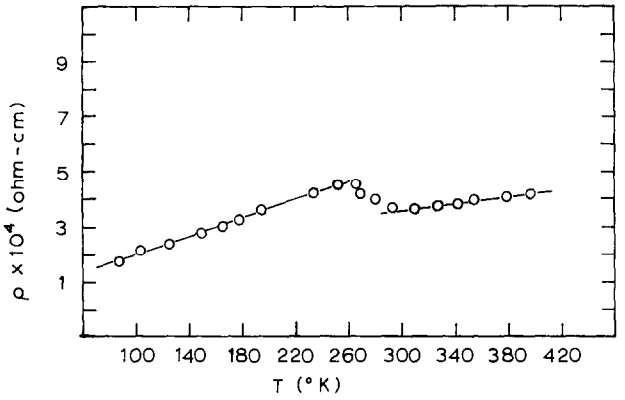

FIG. 2. Resistivity of 2*S*-TaS_2 as a function of temperature.

ohm-cm at 92°K. The resistivity of the 2*S* form was 3.8×10^{-4} ohm-cm at 300°K and 1.8×10^{-4} ohm-cm at 87°K, which may be compared with the values 6.0×10^{-4} ohm-cm at 78°K reported by Van Maaren and Harland (*13*) for mixed-phase samples of TaS_2.

The specular reflectance spectra for both the 1*S* and 2*S* polymorphs are shown in Figs. 3 and 4, respectively. Although the analyses of the absorption components of these spectra are not complete, it is evident that the positions of the minima in these plots correspond closely to the absorption *maxima* in the compounds. The energy transitions corresponding to these absorption maxima are listed in Table II. The spectrum for 2*S*-TaS_2 in Figure 4 resembles those reported by Wilson and Yoffe (*3*) and by Bachman, Kirsch, and Geballe (*14*) for the 2S form of $NbSe_2$. The absorption minimum at E_5 occurs near the plasma frequency. The relatively featureless region below 1 eV in photon energies (above 12,000 Å) is the result of the increase in free carriers. The peak at E_6 is identical in both forms and may be the result of an impurity common to both. In the absence of an analysis of the complex refractive index of those strongly absorbing crystals, assign-

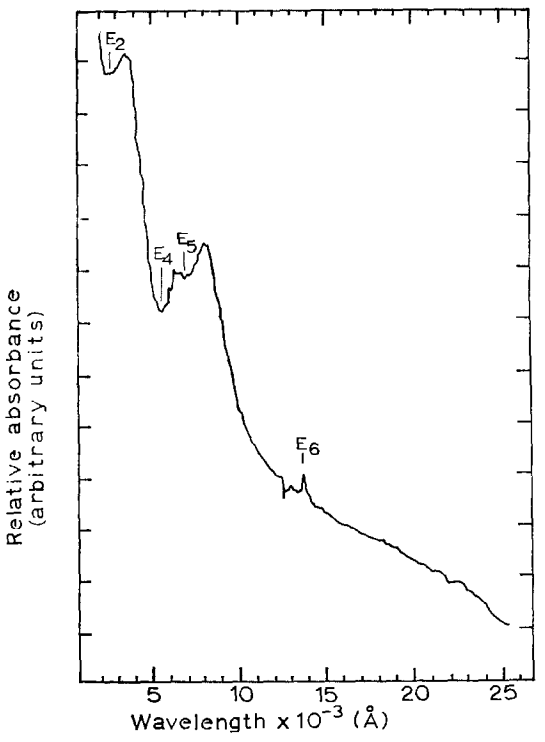

FIG. 3. Specular reflectance spectrum of 1*S*-TaS_2.

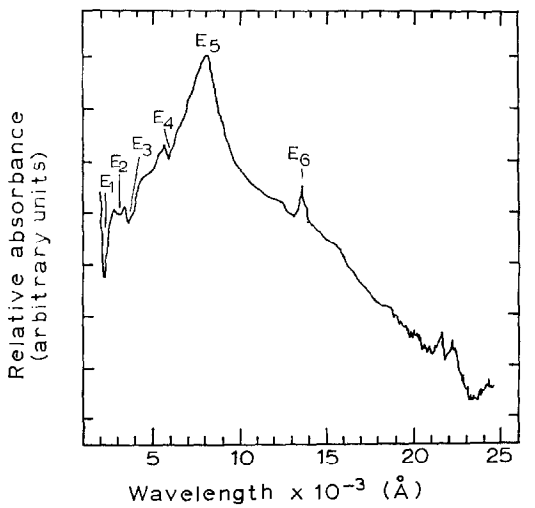

FIG. 4. Specular reflectance spectrum of 2S-TaS_2.

TABLE II

TRANSITION ENERGIES FOR 1*S*-TaS_2 AND 2*S*-TaS_2 FROM SPECULAR REFLECTANCE MEASUREMENTS

	Energy transition (eV)					
Compound	E_1	E_2	E_3	E_4	E_5	E_6
1*S*-TaS_2	—	5.1	—	2.2	1.55	0.89
2*S*-TaS_2	5.7	4.1	3.5	2.1	1.55	0.90

ments of any absorption bands can be only tentative.

A band model for trigonal prismatic coordination of transition metals has been proposed by Huisman, de Jonge, Haas, and Jellinek (*15*), and the energy band diagram for that model is reproduced on the right in Fig. 5. These authors postulate that for 2*S*-TaS_2 the trigonal prismatic coordination (symmetry D_{3h}) of the metal produces a ligand field splitting of the *d* orbitals into the antibonding levels $a_1'^*(d_{z^2})$, $e'^*(d_{x^2-y^2}$ and $d_{xy})$, and $e''^*(d_{xz}$ and $d_{yz})$, (*z* being the trigonal axis). In the solid these levels are broadened into narrow energy bands by metal–ligand and metal–metal interactions. Ligand *s* orbitals and metal *p* orbitals similarly give rise to valence and conduction bands that are generally rather broad. In 2*S*-TaS_2, and similar d^1 compounds, the valence band overlaps the narrow nondegenerate $a_1'^*$ band that is partially filled. The existence of this conduction band would result in metallic conductivity. Our electrical, optical, and magnetic data on 2*S*-TaS_2 single crystals, indicating metallic behavior, are consistent with this model. As a tentative interpretation of the reflectance spectrum in Fig. 4, we propose that the absorption minima E_1–E_4 are caused by transitions between the $a_1'^*$ and e^* bands. If the splitting of the e'^* level, due to spin–orbit coupling is similar to that proposed by Huisman et al., for WS_2, the peak at 2.1 eV (E_4) may be due to transitions to the upper half of the $e_1'^*$ band. The higher energy transitions E_1 and E_2 could then be assigned to the transitions between $a_1'^*$ and e''^* bands. The absorptions below 1 eV are probably due to free carriers.

A schematic energy level diagram for the distorted octahedral structure of the 1*S*-type dichalcogenides was proposed by Vellinga, de Jonge, and Haas (*16*) and is reproduced on the left in Fig. 5. For trigonally distorted octahedral coordination, with the metal atom shifted along the trigonal axis (symmetry C_{3v}), the ligand field splitting produces two degenerate e^* levels and a nondegenerate a^* (d_{z^2}) level with one of the e^* levels being lowest. Employing this model, Vellinga, de Jonge, and Haas have successfully explained the metallic behavior of β-$MoTe_2$, which is isostructural with 1*S*-TaS_2 ($c/a = 1.89$ in

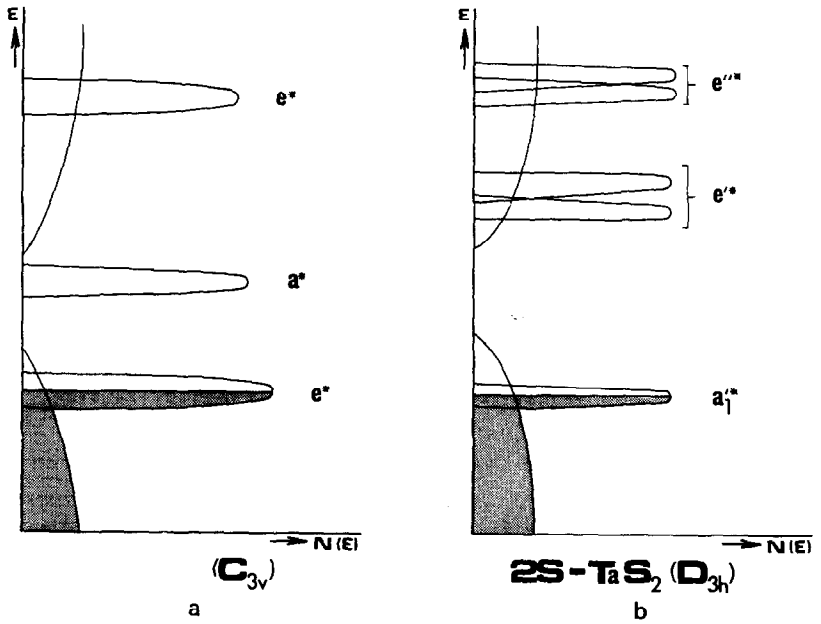

FIG. 5. Schematic one-electron energy level diagrams for the dichalcogenides of transition metals in Groups V and VI (a) with trigonally distorted octahedral (C_{3v}) coordination, (b) with trigonal prismatic (D_{3h}) coordination. Diagram (b) is consistent with the properties of 2*S*-TaS_2, but diagram (a) is not consistent with the semiconductor properties of 1*S*-TaS_2.

β-$MoTe_2$, $c/a = 1.76$ in 1*S*-TaS_2). In the case of the d^2 Mo ions, the degenerate lower e^* level is only half-filled, and metallic conduction results. However, application of this model to d^1 Ta in 1*S*-TaS_2 would again predict an unfilled lower e^* level and metallic properties, in contrast with the experimentally observed semiconductor properties. Wilson and Yoffe (Ref. *3*, p. 299) have suggested that electron–electron correlation in the *d* band results in the formation of electron-hole pairs, a situation that would presumably produce diamagnetic semiconductor behavior in the crystal. These latter authors also cite electron diffraction evidence for a hexagonal supercell in the structure of 1*S*-TaS_2. In agreement with their observation, we have been unable to detect any evidence for such a supercell in X-ray diffraction photographs of our 1*S*-TaS_2 crystals, so that the question of whether or not the electron diffraction evidence is representative of the structure in the bulk of the crystal remains open. An attractively simple alternative is to describe 1*S*-TaS_2 by a quasilocalized electron model consisting of $[TaS_2]^+$ and $[TaS_2]^-$ complexes containing nominally pentavalent (d^0) and trivalent (d^2) tantalum, respectively. The existence of such pairs of ions, or clusters of such pairs, should be evident as a superlattice structure in the crystal, but would require that the supercell contain an even number of TaS_2 stoichiometric molecules. The electron diffraction supercell, cited above, incorporates nine basic cells in a cluster parallel to the *a* plane, but no evidence is available concerning a *c*-axis parameter for a multiple cell. If the complex cluster model were to be consistent with the electron diffraction data, the length of the supercell *c*-axis must be an even multiple of the basic cell parameter. Such a localized model would require that the overlap of molecular orbitals between ions, or clusters of ions, be exceedingly small; so that localized molecular energy levels exist separated by a small energy gap, of the order of 0.1 eV in this case, from the conduction band. An additional constraint on this localized model arises when the diamagnetism of 1*S*-TaS_2 is considered. Since the trigonal ligand field splitting for the metal produces a doubly degenerate lower e^* level, it is necessary to postulate a further splitting of this level in order to rationalize a diamagnetic state for the d^2 trivalent tantalum. No evidence for antiferromagnetism is found in the magnetic data.

Whatever the merits of the various bonding models that are proposed, the TaS_2 system remains an extremely interesting example of a compound that seems to span the Mott transition in two polymorphs. It is also interesting to contrast the transport properties of 1*S*-TaS_2 with those of the isostructural VSe_2. The latter is reported by Hulliger (*17*) to be a metallic conductor with a localized magnetic moment whereas 1*S*-TaS_2 is a nearly diamagnetic semiconductor. Hulliger has noted that in an isomorphous series of compounds the nonmetallic character is weakened on replacing the anion by a heavier element in the same group of the periodic table or by substituting the transition metal by a lighter element from its group. Also, one notes that VSe_2 does not superconduct and, as reported above, 1*S*-TaS_2 does, so that a significant difference in the density of electronic states in the conduction band must exist in these two compounds.

Acknowledgment

It is a pleasure to acknowledge support of this research by the U.S. Army Research Office (Durham).

References

1. F. Jellinek, *J. Less-Common Metals* **4**, 9 (1962).
2. G. Hägg and N. Schönberg, *Ark. Kemi* **7**, 371 (1954).
3. J. A. Wilson and A. D. Yoffe, *Advan. Phys.* **18**, 193 (1969).
4. M. H. Van Maaren and G. M. Schaeffer, *Phys. Lett.* **20A**, 131 (1966).
5. H. Schäfer, "Chemical Transport Reactions," Academic Press, New York, 1964.
6. L. E. Conroy and K. C. Park, *Inorg. Chem.* **7**, 459 (1969); or see L. E. Conroy, *Inorg. Synth.* **12**, 158 (1970).
7. J. J. Lingane, *J. Amer. Chem. Soc.* **67**, 919 (1945).
8. R. W. Moshier, "Analytical Chemistry of Niobium and Tantalum," p. 121, Macmillan, New York, 1964.
9. G. Norwitz, M. Codell, and J. J. Mitula, *Anal. Chim. Acta* **11**, 173 (1954).
10. M. Cohen, *Rev. Sci. Instrum.* **6**, 68 (1935).
11. L. Van der Pauw, *Phillips Res. Rep.* **13**, 1 (1958).
12. M. H. Van Maaren and G. M. Schaeffer, *Phys. Lett.* **24A**, 645 (1967).
13. M. H. Van Maaren and H. B. Harland, *Phys. Lett.* **29A**, 571 (1969).
14. R. Bachman, H. C. Kirsch, and T. H. Geballe, *Solid State Commun.*, **9**, 57 (1971).
15. R. Huisman, R. de Jonge, C. Haas, and F. Jellinek, *J. Solid State Chem.* **3**, 65 (1971).
16. M. B. Vellinga, R. de Jonge, and C. Haas, *J. Solid State Chem.* **2**, 299 (1970).
17. F. Hulliger, *Helv. Phys. Acta* **34**, 1191 (1963); *Phys. Lett.* **5**, 226 (1963).